Electronic Supplementary Material (ESI) for New Journal of Chemistry.

Fluorooxoborate Layers： Second Harmonic Generation and Raman Spectra Anisotropy

Abudukadi Tudi [a,b†], Shujuan Han [a†], Zhihua Yang [*a], Shilie Pan [*a]

[a]CAS Key Laboratory of Functional Materials and Devices for Special Environments, Xinjiang Technical Institute of Physics & Chemistry, CAS; Xinjiang Key Laboratory of Electronic Information Materials and Devices, 40-1 South Beijing Road, Urumqi 830011, China.

[b]Center of Materials Science and Optoelectronics Engineering, University of Chinese Academy of Sciences, Beijing 100049, China.

To whom correspondence should be addressed :

E-mail: slpan@ms.xjb.ac.cn (Shilie Pan).

E-mail: zhyang@ms.xjb.ac.cn (Zhihua Yang)

Contents

Calculations details and methods

Properties of fluorooxoborate and KBBF functional layers were obtained on the basis of *ab initio* calculations implemented in the CASTEP package through density functional theory (DFT).[1] The generalized gradient approximation (GGA) [2] was adopted, and Perdew-Burke-Ernzerhof (PBE)[3] functional was chosen to calculate the exchange-correlation potential, with an energy cutoff of 780 eV under the Norm conserving pseudopotentials. The numerical integration of the Brillouin zone was performed using a 3 ×3 ×1 Monkhorst-Pack k-point sampling. We set the layer in the *xy* plane, and adopted a 20 Å supercell length in the z direction to avoid the interaction between the layers.

The SHG anisotropy of functional layers in C_1, C_{2v} and C_3 point groups can be calculated by the following equations:

$$I_{C_1}^{\parallel} = |d_{11}\cos^3\theta + (d_{12} + 2d_{26})\cos\theta\sin^2\theta + (2d_{16} + d_{21})\cos^2\theta\sin\theta + d_{22}\sin^3\theta|^2 \quad (1)$$

$$I_{C_s}^{\perp} = |d_{12}\sin^3\theta + (d_{22} - 2d_{16})\cos\theta\sin^2\theta + (2d_{26} - d_{11})\cos^2\theta\sin\theta - d_{21}\sin\cos^3\theta|^2 \quad (2)$$

$$I_{C_{2v}}^{\parallel} = |d_{22}\sin^3\theta + (d_{16} + 2d_{21})\sin\theta\cos^2\theta|^2 \quad (3)$$

$$I_{C_{2v}}^{\perp} = |d_{21}\cos^3\theta + (d_{22} - 2d_{16})\cos\theta\sin^2\theta|^2 \quad (4)$$

$$I_{C_3}^{\parallel} = |d_{22}\sin^3\theta - 2d_{22}\sin\theta\cos^2\theta|^2 \quad (5)$$

$$I_{C_3}^{\perp} = |2d_{22}\cos\theta\sin^2\theta - d_{22}\cos^3\theta|^2 \quad (6)$$

Raman scattering intensities of C_1, C_{2v} and C_3 point groups can be calculated as following equations:

C_1: $S_{A_g}^{\parallel} = |a\cos^2\theta + b\sin^2\theta + 2d\sin\theta\cos\theta|^2$ (7)

$$S_{A_g}^{\perp} = |d\cos^2\theta - d\sin^2\theta + (b-a)\sin\theta\cos\theta|^2 \quad (8)$$

C_{2v}:

$$S_{A_{1g}}^{\parallel} = |a\cos^2\theta + b\sin^2\theta|^2 \quad (9)$$

$$S_{A_{1g}}^{\perp} = |b\sin\theta\cos\theta - a b\sin\theta\cos\theta|^2 \quad (10)$$

$S^{\parallel}_{A_{2g}} = |2dsin\theta cos\theta|^2$ (11)

$S^{\perp}_{A_{2g}} = |d\cos^2\theta - d\sin^2\theta|^2$ (12)

C_3 :

$S^{\parallel}_{A_g} = |a\cos^2\theta + a\sin^2\theta|^2$ (13)

$S^{\perp}_{A_g} = 0$ (14)

$S^{\parallel}_{1E_g} = |ccos^2\theta - csin^2\theta + 2dsin\theta cos\theta|^2$ (15)

$S^{\perp}_{1E_g} = |dcos^2\theta - dsin^2\theta - 2csin\theta cos\theta|^2$ (16)

$S^{\parallel}_{2E_g} = |dcos^2\theta - dsin^2\theta - 2csin\theta cos\theta|^2$ (17)

$S^{\perp}_{2E_g} = |csin^2\theta - ccos^2\theta - 2dsin\theta cos\theta|^2$ (18)

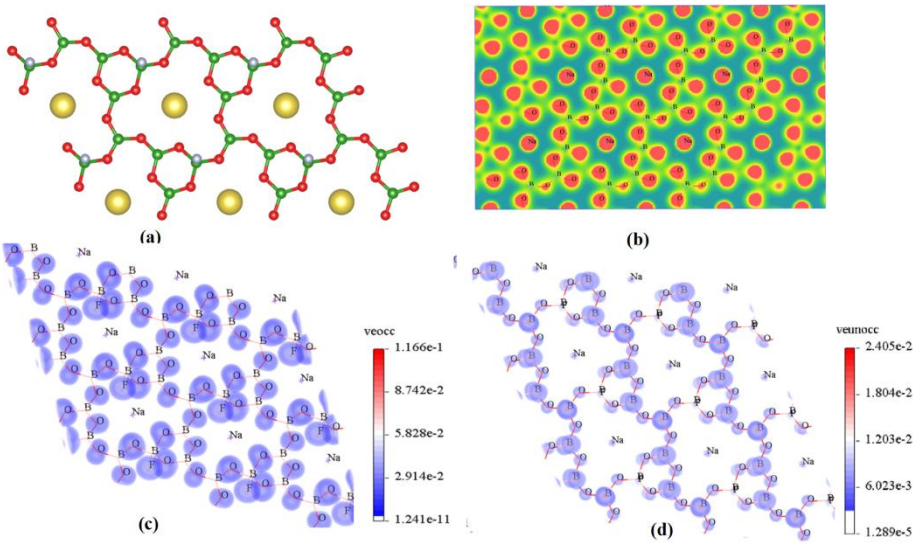

Fig. S1 (a) The NaB_4O_6F layer, (b) the electronic density of NaB_4O_6F layer. The SHG densities of the NaB_4O_6F layer, (c) virtual-electron (VE) occupied states and (d) VE unoccupied states.

The highlighted electronic density of the NaB_4O_6F layer shows the anisotropy of bonding electron distributions of the B-O-F layer, which indicates its significant role in the birefringence (Fig. S1b). The SHG-density of virtual-electron(VE) occupied (veocc) and unoccupied (veunocc) states are shown in Fig. 1c, 1d. For the occupied states, O-2*p* and F-2*p* orbitals make significant contribution to the SHG effects. In unoccupied states, the B-2*p*, O-2*p* and F-2*p* orbitals contribute to the SHG response. Therefore, the NaB_4O_6F layer plays a key role both in SHG response and birefringence, which exhibits the characteristic of functional layers for the nonlinear optical performances.

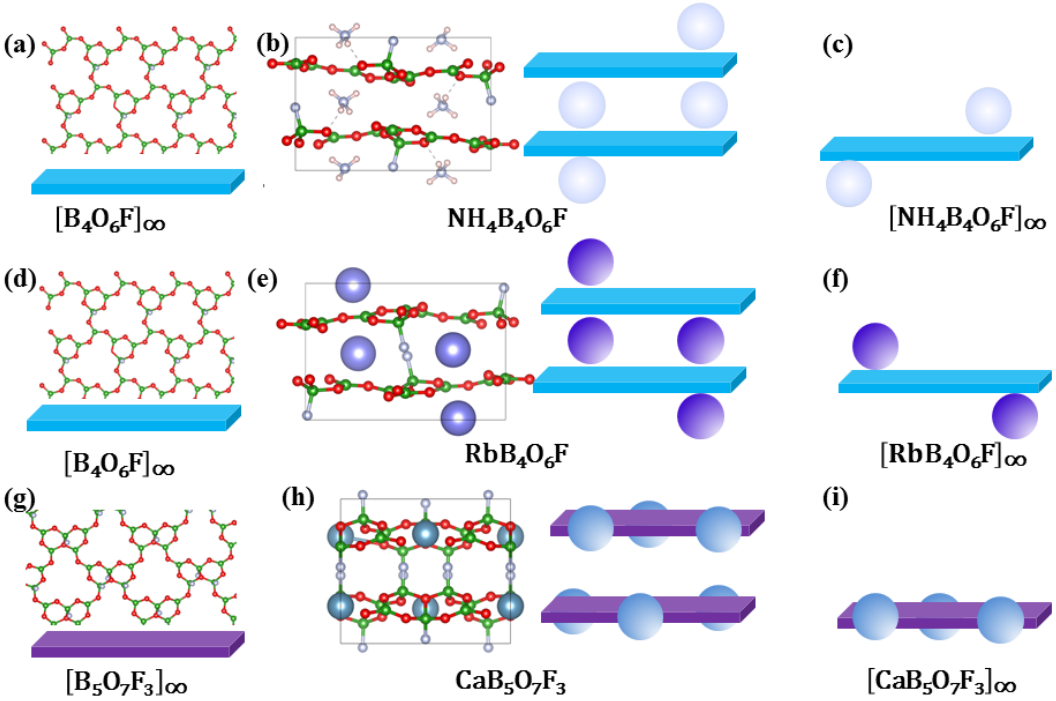

Fig. S2 (a) The $[B_4O_6F]_\infty$ functional layer, (b) the unit cell of $NH_4B_4O_6F$, (c) the $[NH_4B_4O_6F]_\infty$ layer, (d) the $[B_4O_6F]_\infty$ functional layer, (e) the unit cell of RbB_4O_6F, (f) the $[RbB_4O_6F]_\infty$ layer, (g) $[B_5O_7F_3]_\infty$ functional layer, (h) the unit cell of CaB_5O_7F, (i) the $[CaB_5O_7F_3]_\infty$ layer.

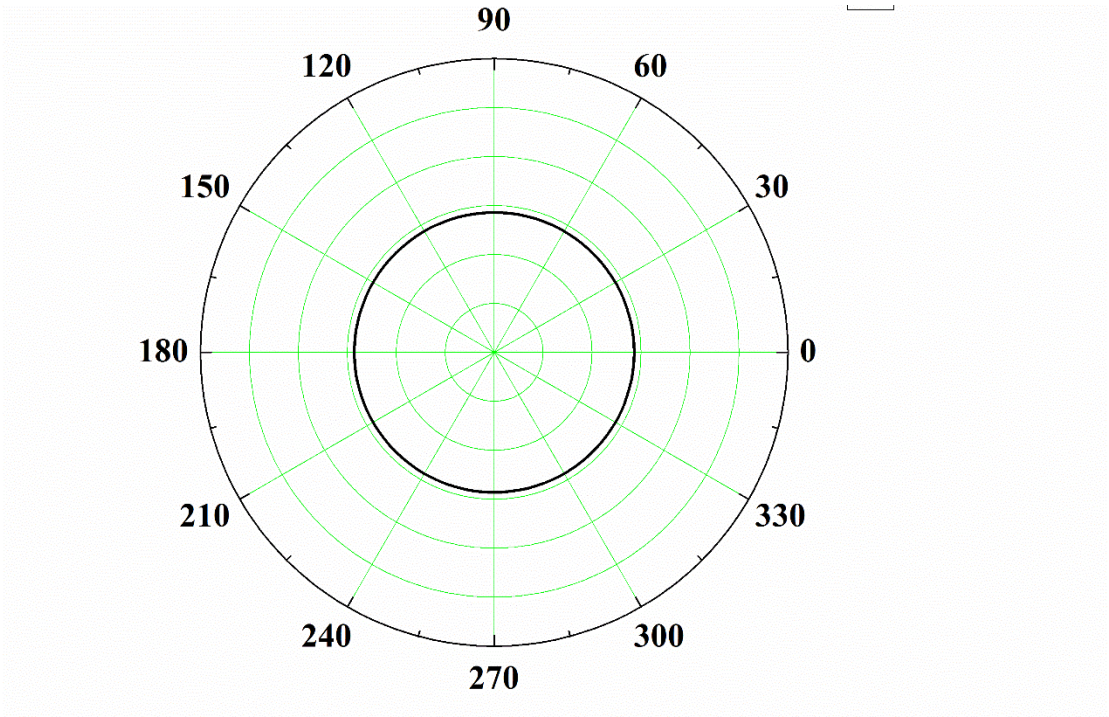

Fig. S3. The angle dependence of the Raman intensities under parallel polarization configurations of the KBBF functional layer (A_g modes).

References

1 S. J. Clark, M. D. Segall, C. J. Pickard, P. J. Hasnip, M. J. Probert, K. Refson and M. C. Payne, *Z. Kristallogr.*, 2005, **220**, 567.

2 J. P. Perdew, K. Burke and M. Ernzerhof, *Phys. Rev. Lett.*, 1996, 77, 3865.

3 A. M. Rappe, K. M. Rabe, E. Kaxiras and J. D. Joannopoulos, *Phys. Rev. B*, 1990, **41**, 1227.